Spray Dried Aerosol Particles of Pyrazinoic Acid Salts for Tuberculosis Therapy

P.G. Durham[1], Y. Zhang[1], N. German[1,2], N. Mortensen[1], J. Dhillon[3], D.A. Mitchison[3], P.B. Fourie[4] and A.J. Hickey[1]*

[1]RTI International, Research Triangle Park, NC27709, USA,

[2]Currently, School of Pharmacy, Texas Tech. University Health Sciences Center, Amarillo, TX79106, USA

[3]St George's Hospital, University of London, UK

[4]Department of Medical Microbiology, University of Pretoria, South Africa,

*Author for correspondence

ABSTRACT

Tuberculosis is the most serious infectious disease caused by a single organism, *Mycobacterium tuberculosis (Mtb)*. The standard of care is a protracted and complex drug treatment regimen made more complicated and of longer duration by the incidence of multiple- and extensively drug resistant disease. Pulmonary delivery of aerosols as a supplement to the existing regimen offers the advantage of delivering high local drug doses to the initial site of infection and most prominent organ system involved in disease. Pyrazinamide is used in combination with other drugs to treat tuberculosis. It is postulated that the action of pyrazinoic acid (POA), the active moiety of pyrazinamide, may be enhanced by local pH adjustment, when presented as a salt form. POA was prepared as leucine (POA-leu) and ammonium salts (POA-NH4), spray dried and characterized in terms of physico-chemical properties (melting point, crystallinity, moisture content), aerodynamic performance (aerodynamic particle size distribution, emitted dose) and in vitro inhibitory effect on two mycobacteria (*Mtb* and *Mycobacterium bovis*) . Particles were prepared in sizes suitable for inhalation (3.3 and 5.4μm mass median aerodynamic diameter and 61 and 40% of the aerodynamic particle size distribution less than 4.46μm, as measured by inertial impaction, for POA-leu and POA-NH4, respectively) and with properties (stoichiometric 1:1 ratio of salt to drug, melting points at ~180°C, with water content of <1%) that would support further development as an inhaled dosage form. In addition, POA salts demonstrated greater potency in inhibiting mycobacterial growth compared with POA alone which is promising for therapy.

INTRODUCTION

More than 9 million cases of tuberculosis (TB), with 1.5 million deaths, occur each year [1] despite the availability of effective treatment. The standard of care for TB in most high-burden regions is a six month regimen, in which the initial 2 months include isoniazid (INH), rifampicin (RIF), pyrazinamide (PZA) and ethambutol (E), followed by a 4 month continuation phase of RIF and INH (underlined letters used as abbreviations for courses shown below). The introduction of RIF and PZA into TB therapy allowed the duration of treatment to be reduced from at least 12 months to 6 months with <5% relapses. However, further reductions in the duration of treatment resulted in increasing rates of relapse after completion of treatment [2]. In the absence of a new more efficacious regimen, there is general agreement that shortening the duration of treatment with the current regimen from 6 months to 3 months or less would be a useful improvement since it would reduce the burden of lengthy treatment and the supervision of drug-taking for the patients and for the clinic, as well as diminishing the emergence of drug resistance. Indeed, at a recent meeting of the TB Union the importance of shortening the duration of therapy was identified [3]. While we wait for the advent of affordable new drugs, a way forward to improve the efficacy of treatment of pulmonary TB and shortening its duration is to improve the performance of the two drugs, RIF and PZA, that are together responsible for almost all of the bactericidal action of the 2EHRZ/4RH regimen [4]. The subject of PZA in TB therapy has recently become the focus for discussion and exploration, providing a rationale for the studies described here [3, 5-8].

Tuberculosis is acquired by entry of *Mycobacterium tuberculosis (Mtb)* by the pulmonary route. In addition, throughout disease progression the lung is a primary site of infection. Upon deposition in the lungs Infectious organisms are taken up by macrophages as depicted in Figures 1a and b. The mechanism of action of PZA and POA should be considered in order to characterize the outcome of lung delivery with respect to treatment of infection.

PZA was introduced by Lederle and Merck [9, 10] in the early 1950s as a result of its high activity in experimental murine TB. Following a small clinical study on its use in treating patients [11, 12], it was then studied at Cornell University using the long term mouse model [12]. Mice were infected and treated with a combination of PZA with INH, to prevent rapid emergence of PZA resistance [13]. As treatment progressed, counts of viable *M. tuberculosis* in the spleens of mice treated with INH+PZA decreased in parallel to the counts on the control mice treated with INH, streptomycin, and p-aminosalicylic acid (PAS) for the first 2-3 weeks, but continued downwards eventually to no colonies on culture while the counts on the control culture gradually decreased to a constant proportion of surviving persisters. Further clinical development of pyrazinamide showed that at appropriate doses, PZA could substantially accelerate the progress of chemotherapy [14].

PZA was shown in 1967 to be a pro-drug that was converted to the active molecule POA by the amidase of M. tuberculosis [15]. POA itself was not absorbed from the gastrointestinal tract (GI). A more detailed description of the mode of action of PZA has been provided recently by Zhang who had access to labeled PZA and could, therefore, track the movement of PZA and POA within and in the immediate surroundings of the bacilli [16]. In a series of publications, Zhang developed a hypothesis illustrated in Figure 1d. In this, the PZA is first de-aminated within the cytoplasm of *Mtb* being converted to –NH3 and POA by the amidase pncA [17]. The POA then leaves the bacterial cell and, if the local environment is acidic, re-enters the cell by passive diffusion in a highly pH dependent manner according to the Henderson-Hasselbach equation. Once in the cell, the POA can only escape with the help of an inefficient, energy dependent, efflux pump. Thus, if there is only a small energy pool available to run the inefficient pump, POA will tend to accumulate within the cell and eventually kill it. The mechanism may involve damage to the cell membrane. Since bacteria that persist are likely to have low energy pools, they are particularly liable to be killed by PZA.

The natural route of infection of TB is via inhalation of bacilli-containing aerosols. The bacilli settle in the deep lung, where they are phagocytized by alveolar macrophages, ultimately resulting in pulmonary TB infection. Targeted delivery of anti-TB therapies directly to infected lungs results in immediate contact of the drug with the TB bacteria, leading to high local drug concentrations and rapid onset of killing action. A smaller dose combined with the absence of first pass metabolism is expected to lead to reduced systemic side effects and ultimately enhanced patient compliance to the treatment, compared to the orally-delivered regimen. Particles deposit in the lung by inertial impaction, sedimentation and diffusion [18, 19]. Large particles (aerodynamic diameter, $d_a > 5$ μm) tend to deposit by impaction in the extra-thoracic cavities, smaller particles (d_a = 1–5 μm) deposit deeper in the lungs by inertial impaction and sedimentation, while very small particles ($d_a < 1$ μm) are driven by diffusion, mostly remain suspended, and are ultimately exhaled. A number of anti-TB drugs have been formulated in dry powder microparticles for pulmonary delivery, including capreomycin [20, 21] and paraaminosalicylic acid [22]. Indeed, these studies indicated that direct delivery to the lungs results in high local concentrations and reduced bacterial burden compared to the same treatments delivered via other routes, offering the possibility of both reduced doses and reduced systemic side effects. The delivery of antitubercular drugs to the lungs has been reviewed thoroughly elsewhere [23, 24].

It is proposed that aerosol particles containing POA salts delivered to the lungs (Figure 1a) in sizes that would facilitate peripheral deposition (Figure 1b) where macrophage uptake (Figure 1c) would bring the drug proximal to the micro-organism will enhance therapeutic effect (Figure 1d).

Figure 1. The role of POA salt (POA-leucine and POA-NH4) in elevating the bactericidal activity of PZA, and bypassing resistance. a) POA salts are manufactured and aerosolized into microparticles. b) Inhaled microparticles are deposited in the alveolar, c) where the microparticles are phagocytosed by macrophages infected with M. tuberculosis. d) Inside macrophages, microparticle dissolves and the POA salt modulates local pH increasing the activity of PZA.

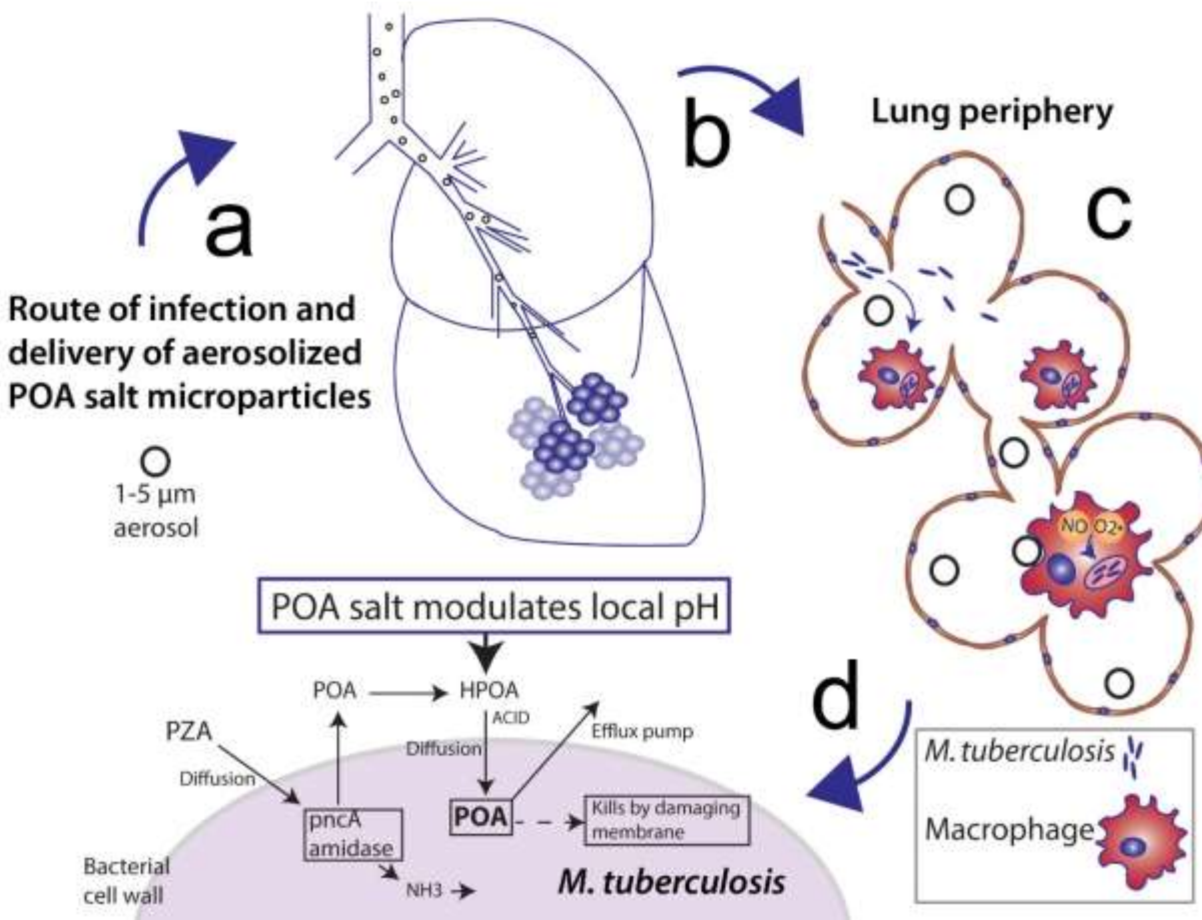

The novelty of the work described consists of: (a) The use of POA as a candidate for tuberculosis therapy; (b) its preparation as a salt which is justified by a hypothesis that has previously not been addressed and; (c) preparation of the salt as a particulate dosage form to capitalize on local delivery to the lungs.

MATERIALS

POA was purchased from Sigma Aldrich, L-leucine was purchased from Fluka and ammonium hydroxide was purchased from Fisher Scientific.

Nuclear magnetic resonance demonstrated the presence of stoichiometric 1:1 ratios of POA to leucine and ammonium ion in each of the salt forms. The weight percentage by elemental analysis was within ±0.4%, confirming the exact stoichiometric ratios.

METHODS

Pyrazinecarboxylic acid (1.00 g, 8.05 mmol) and L-leucine (1.06g, 8.05 mmol) were suspended in water (50 mL). The reaction mixture was heated to 60 °C and stirred until the reaction mixture became clear. The solution was cooled to room temperature and the solvent was removed under vacuum. The resulting salt was collected and dried on high vacuum for an extensive period of time (1 week) to give the desired product as a white powder in quantitative yield (2.06 g).

Pyrazinecarboxylic acid (4.0 g; 32.2 mmol) was suspended in water (30 mL) and aqueous ammonium hydroxide (4.52 mL; 38.7 mmol) was added drop wise to the reaction mixture. The reaction was stirred for 30 minutes and a clear homogeneous solution was obtained. The solvent was removed under vacuum to provide a white solid. The resulting solid was suspended in methanol (50 mL) and stirred at room temperature for 2 hours to assist to remove the excess ammonium hydroxide. The final salt was collected by filtration and dried on high vacuum for an extensive period of time (1 week) to give final product as a white powder in quantitative yield (4.54 g).

Salt Characterization

^{1}H NMR: ^{1}H NMR spectra were recorded on a Bruker Avance DPX-300 (300 MHz) spectrometer. Around 5 mg of each salt was dissolved in 0.7 ml of an appropriate deuterated solvent (deuterated water for leucine salt and deuterated dimethyl sulfoxide for ammonium salt) and submitted immediately to NMR analysis. Chemical shifts are reported in ppm relative to the reference signal and coupling constant (J) values are reported in hertz (Hz).

Elemental analysis: Approximately 10 mg of each salt was analyzed by Atlantic Microlab, Inc. (Georgia, US). The elements carbon, nitrogen, and hydrogen were analyzed by combustion using automatic analyzers. All results are presented as percent by weight determinations.

Hot Stage Microscopy. Samples were prepared and analyzed using a capillary melting point apparatus (Mel-Temp II, Laboratory Devices, Inc., Holliston, MA). Each salt was powdered and placed in thin-walled capillary tube (1 mm diameter, 10 cm height) in the heating chamber of the melting point apparatus. In order to first determine the melting point range, the initial melting experiment was run with the starting temperature at 25 ^{o}C and ramping rate was set to ensure a steady increase of ~5 ^{o}C/min. For precise measurements a second melting experiment was performed with the starting temperature at 10 ^{o}C below the melting point range previously determined and a ramping rate at 2 ^{o}C/min was employed.

Particle Manufacture

Aqueous solutions of the salts were prepared by dissolution in ultrapure water (resistivity = 18.2 MΩ-cm, Barnstead NanoPure, Thermoscientific, Waltham, MA) at a mass concentration of 10 mg/mL, with solutions having pH of 2.70 ± 0.02 and 4.56 ± 0.02 for POA-leu and POA-NH4 respectively (SympHony, VWR, Radnor, PA). Solutions were spray dried (Model B-290, Buchi, Falwil, Switzerland) in an open loop configuration, with a two-fluid nozzle of inner and outer orifice diameters 0.7 and 1.5 mm, respectively. Ultra-high purity nitrogen was employed as the atomizing gas. The aspirator was operated at 35 m^3/hour capacity. The solution was introduced by a peristaltic pump at a flow rate of 6.5 mL/min, while atomizing gas was adjusted to flow rates between 439 – 1052 liters/hour. The inlet temperature was 140°C, corresponding to an outlet temperature of 80°C. Powders were removed from the collection vessel and stored in amber glass vials over desiccant at room temperature. Recovery was determined gravimetrically with respect to nominal mass spray dried (400mg).

Particle Characterization

Morphology: Particle morphology after spray drying was evaluated by scanning electron microscopy (Quanta 200, FEI, Hillsboro, OR). Powder was sampled onto an adhesive carbon substrate mounted on an aluminum sample holder and sputter coated with gold/palladium (Hummer Sputtering System, Anatech Ltd, Union City, CA) for a period of 120 seconds. Images of POA salts were captured.

X-Ray Powder Diffraction (XRPD): POA alone, POA-NH4 and POA-leu before and after spray drying were evaluated (XRD-600, Shimadzu, Japan). Powder was loaded into a glass sample holder, packed to uniform geometry and analyzed from 5-70° 2ϴ at an interval of 0.02° 2ϴ with a dwell time at each step of 2 seconds without rotation, and a slit arrangement of 1 degree for the divergence and scatter slits. X-ray beam source was a copper anode operated at 45 kV and 40 mA.

Thermal Analysis: Two methods were employed to evaluate the powder thermal properties. POA alone, POA-NH4 and POA-leu before and after spray drying (denoted hereafter as “SD”) were evaluated.

Thermogravimetric analysis: Salts were analyzed (TGA Q50, TA Instruments, New Castle, DE) for moisture loss and thermal decomposition by placing in a platinum sample pan and heating at a rate of 2°C/min from 20°-300°C and a sample mass of approximately 5mg with nitrogen purge at 60 mL/min.

Differential Scanning Calorimetry: Samples were analyzed (Q200, TA Instruments, New Castle, DE) for phase transitions in response to heating by placing in aluminum pans, crimping and using a ramp rate of 5° C/min.

Residual Moisture Determination by Karl Fischer Titration: Powders were analyzed after spray drying for water content by Karl Fischer titration on a Mettler Toledo V30 Compact Volumetric Karl Fischer Titrator using 3-5 mg per replicate (n=3).

Aerodynamic Particle Size Distribution (APSD): Mass median aerodynamic diameter (MMAD) was determined by inertial impaction using a Next Generation Impactor (NGI) (MSP Corporation, Minneapolis, MN). The impactor was operated with preseparator and at a flow rate of 60 L/min, a standard practice for evaluating dry powder inhaler performance [25]. Each of the spray dried POA salt powders (10 mg) was loaded into

#3 hydroxypropylmethylcellulose (HPMC) capsules (Quali-V, Qualicaps, Whitsett, NC) and delivered (3x) to the impactor from a Cyclohaler dry powder inhaler (Plastiape, Osnago LC, Italy) which has a pressure drop of 16.4 mBar at 60 L/min [26]. Impactor stages were coated with silicone oil to minimize particle bounce with the exception of the micro-orifice collector plate. Samples were recovered from stages with deionized water and solutions were assayed spectrophotometrically at a wavelength of 268nm (SynergyMX, Biotech, Winooski, VT). MMAD was calculated computationally by plotting cumulative percent by mass of particles undersize against respective stage cutoff diameter and applying a log-linear fit of two points on either side of 50% cumulative mass [27] to identify the median. The geometric standard deviation was estimated from the square root of the ratio of the particle size defined by the 84th percentile of the distribution with respect to the particle size defined by the 16th percentile of the distribution.

Emitted dose: Each of the POA salt powder aerosols was sampled through a glass fiber filter using sampling apparatus B designated in USP <601> [25] operated at 60 L/min with 10mg capsules loaded as previously stated. Filter and apparatus interior were washed and subsequently assayed by UV-Vis. Emitted dose was determined as a percentage of emission from one actuation of a 10 mg capsule.

Fine Particle Fraction: Fine particle fraction (FPF < 4.46μm) can be presented as a function of nominal (FPF_N) and emitted dose (FPF_{ED}). The nominal dose is that in the capsule. The FPF_N is the ratio of mass collected on impactor stages 3 through the micro-orifice collector with respect to the nominal dose expressed as a percentage. The FPF_{ED} is the ratio of the mass collected on impactor stages 3 through the micro-orifice collector with respect to the total mass delivered to the impactor including the inlet and the preseparator expressed as a percentage.

Antibacterial activity of POA salts. The antibacterial effect of the POA salts were tested *in vitro* on *Mtb* strain H37Rv (*Mtb* H37Rv) and Bacillus Calmette-Guerin (BCG, attenuated *M bovis*), BCG does not have amidase and, therefore, does not convert PZA to POA salt (Figure 1d). *Mtb* H37Rv and BCG was kept as a stock strain in liquid nitrogen and serially transferred at weekly intervals to 7H9 Broth+ ADC(Becton Dickinson.).

Experimental procedure:

Seven day cultures of *Mtb* H37Rv and BCG were grown in 7H9 broth (pH 6.2) and inoculated at a1: 4 by volume in 30-ml screw cap universals. These cultures were incubated for 60 days undisturbed. At the start of the experiment pH was adjusted to 5.6. using 1M sodium citrate. Samples were taken for viable count (T0). Antibacterial drugs were added at concentrations of 150 mg/L of PZA, POA and each of the two salts. Over a 21-day period of incubation at 37^{o} C, weekly samples were taken and viable counts were determined.

Viable counts: Samples were briefly ultrasonicated to disrupt cell aggregates. Ten fold serial dilutions were made in water and 0.1 ml volume plated onto one-third segment of 7H11 agar+OADC (Becton Dickinson) medium plates. Plates were packed into polyethylene bags and incubated for 3-4 weeks at 37^{o}C before bacteria (colony forming units, CFU). Colony counts were converted to $\log_{10}$ cfu/mL. Four replicates samples were evaluated and means and standard deviations calculated. All work was carried out in Biological Containment Level 3 laboratory according to Health and Safety Act (1974) and COSSH (2004) and are suitable for handling ACDP Hazard group 3 pathogens.

Statistics: T-test and ANOVA were performed to compare the means and the variances between each of the treated and untreated groups. Statistical significance for both tests was defined as $p<0.05$.

RESULTS

Salt Characterization

^{1}H NMR: Chemical shifts were determined for each of the salts. The POA-Leu chemical shifts appeared as follows: (300 MHz, D_2O) δ 9.10 (s, 1H), 8.66 (d, J = 6.0 Hz, 2H), 3.75 (m, 1H), 1.45 – 1.75 (m, 3H), 0.85 (m, 6H). The POA-NH4 chemical shifts appeared as follows: (300 MHz, DMSO-d_6) δ 8.98 (s, 1H), 8.53 (s, 2H), 7.043 (br.s., 3H).

Elemental analysis: Elemental analysis for both salts correlate with the theoretical calculation of equimolar concentrations of POA and respective counterion, as shown in Table 1.

Table 1. Elemental Analysis

POA-leu		
Element	Theoretical	Experimental
C	51.76	51.90
H	6.71	6.94
N	16.46	16.16

POA-NH4

Element	Theoretical	Experimental
C	42.55	42.81
H	5.00	5.05
N	29.77	29.79

***Preliminary Melting point determination**:* Melting point analysis revealed that the leucine salt decomposed at a temperature of 175°C while the ammonium salt melted at 181-183°C.

Particle Characterization

Recovery as a proportion of the initial mass after spray drying of small quantities of POA-leu was 39% and POA-NH4 was 10%.

Particle Morphology: The POA-leu particles, shown in Figure 2a, appeared as collapsed hollow spheres with smooth surfaces and small pores. POA-NH4 particles were mostly spherical with a corrugated surface, as depicted in Figure 2b. The geometric mean diameters were 3.7 ± 1.77 and 4.6 ± 1.87 µm for POA-leu and POA-NH4 respectively, as determined by image analysis (n=100).

X-Ray Powder Diffraction: XRPD data are shown in Figure 3. POA shows a primary peak at 27.69°, with modest but detectable peaks at other angles. POA-leu had dominant peaks in order of intensity at 13.35, 24.36 and 30.57° 2ϴ. POA-leu SD had dominant peaks at 19.05, 19.74, and 27.61° 2ϴ. POA-NH4 had dominant peaks at 12.78, 15.54 and 19.90° 2ϴ. POA-NH4 SD had dominant peaks at 14.24, 19.72 and 27.52° 2ϴ. Peaks were observed for leucine in order of peak intensity at 24.36, 30.56,

Figure 2. Scanning electron micrographs depicting particles resulting from the spray drying of a) POA-leu salt and b) POA-NH4.

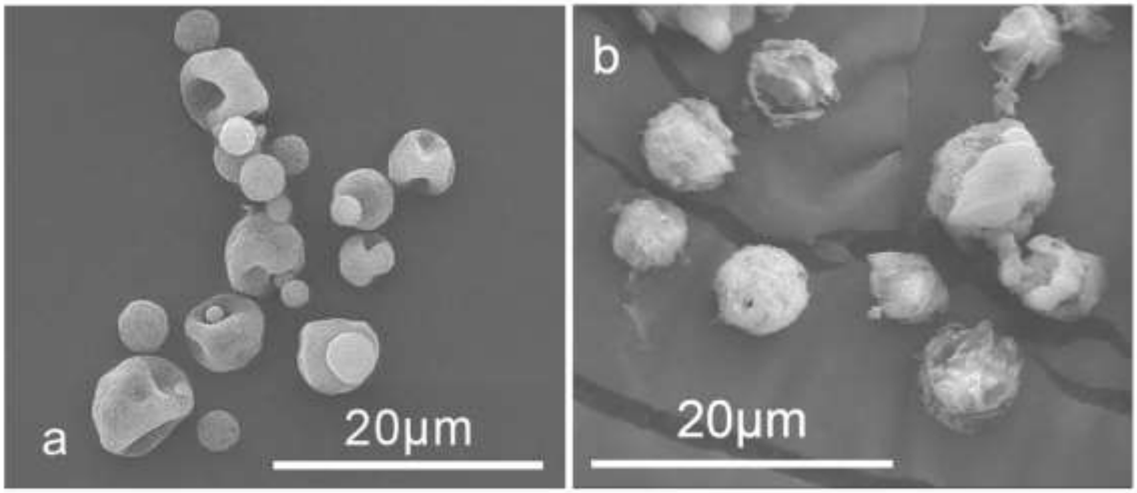

Figure 3. X-ray powder diffraction patterns for a) pyrazinoic acid (POA) and L-leucine and b) pyrazinoate salts before and after spray drying.

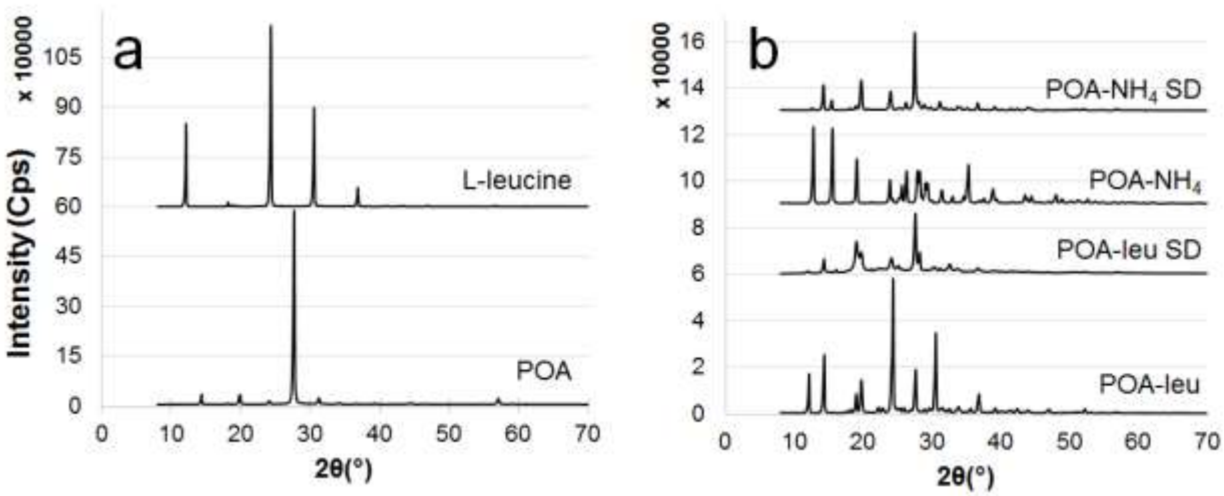

12.12 and 36.84° 2Θ. The intensity for the primary peak for the POA alone was much greater than any of peaks of the salt powders.

Figure 4. Thermogravimetric analysis thermograms for a) POA-leu before and after spray drying, b) POA-leu salt as compared to POA and L-leucine, c) POA-NH4 before and after spray drying, and d) a comparison of POA to both salts.

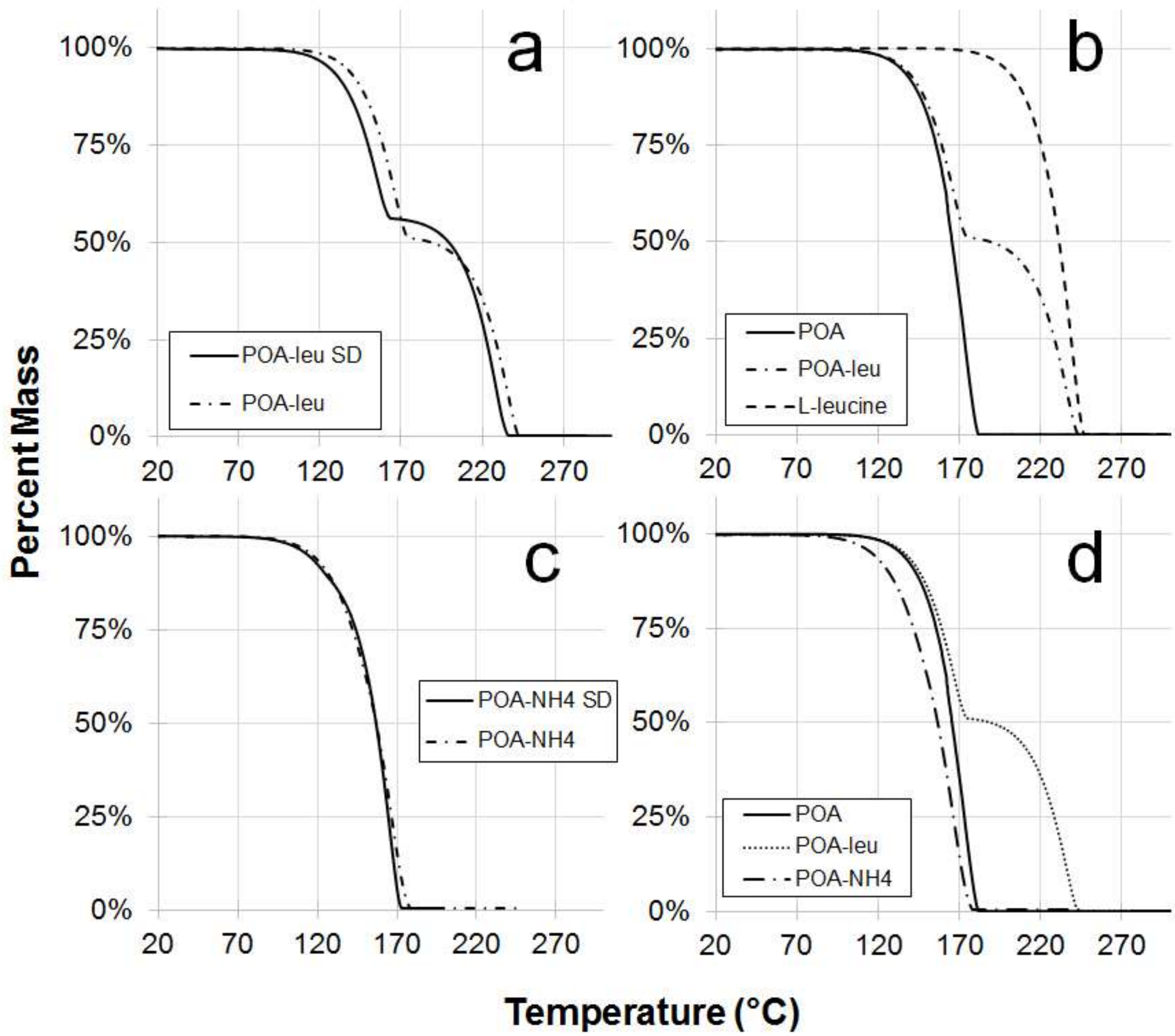

Thermal Analysis

Thermogravimetric analysis: Thermograms are shown in Figure 4. POA-leu displayed a bimodal TGA profile, with onset of the first event occurring at 110°C and culminating at 180°C, and the second event occurring from 180°C to 250°C, as shown in Figure 4a.

Figure 4b shows the behavior of POA and leucine alone as a reference for the inflection observed in the salt thermogram. The TGA curve for POA-NH4 was marked by a single event occurring from 100°C to the loss of all mass at 157°C as shown in Figure 4c. TGA data from the spray dried material closely match those of the starting material, each having little residual solvent. Loss of POA begins at 110°C and culminates at 180°C. Figure 4d compares the profile of POA against both salts. There was no evidence for the presence of moisture at the limit of detection of this method in either powder as would ordinarily be seen as a distinct feature on the thermogram representing mass loss at temperatures slightly below 100° up to 150°C depending on the extent of binding (free or bound).

Figure 5. Differential scanning caliorimetry curves for POA and pyrazinoate salts before and after spray drying.

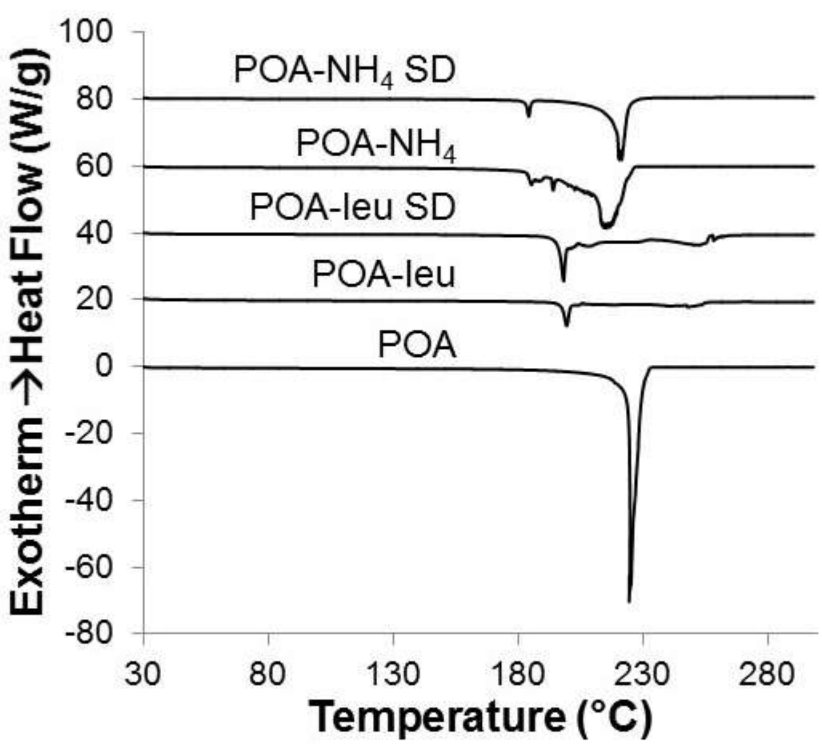

Differential Scanning Calorimetry: Figure 5 depicts the DSC endotherms generated from an evaluation of salts before and after spray drying. It is evident that the melting point of POA (223 °C) was lowered in the salts (POA-leu ~200 °C, POA-NH4, ~180 °C) to approximately the same extent both before and after spray drying. Consequently, there does not appear to be a significant effect of spray drying on the melting point.

Residual Moisture Determination by Karl Fischer Titration: POA-leu and POA-NH4 spray dried powders had an average moisture content of 0.37% ± 0.06 and 0.66% ± 0.43 respectively.

Figure 6. Aerosol particle size distribution depicted as mass deposition per impactor stage for spray dried pyrazinoate salts (n=3, mean ± SD)

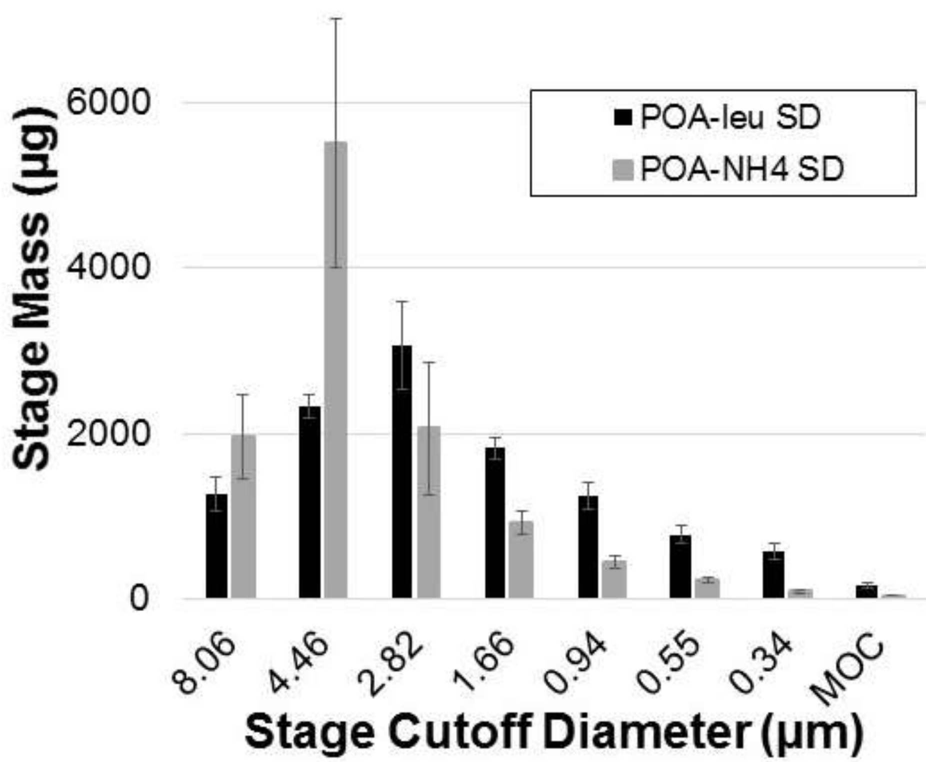

Aerodynamic Particle Size Distribution: Figure 6 shows the APSDs of the two salt forms. POA-leu particles exhibited a MMAD of 3.29 ± 0.05 µm and a GSD of 1.91 ±0.2 (n=3), FPF_N of 44% and FPF_{ED} of 61%. MMAD for POA-NH4 particles was 5.4 µm (GSD 1.83), with FPF_N of 34% and FPF_{ED} of 40%.

Emitted dose: was 71.7 ± 3.4% and 69.8 ± 2.8% for POA-leu and POA-NH4, respectively (n=6).

Figure 7. Bacterial growth inhibition of a) *Mycobacterium tuberculosis* strain H37Rv and b) *Mycobacterium bovis* strain BCG by pyrazinamide, POA and POA-salts as compared to untreated control evaluated over a period of 21 days (n=4, mean ± SD). ANOVA and t-test, statistical significance ($p<0.05$) * compared to untreated control, **compared to POA alone

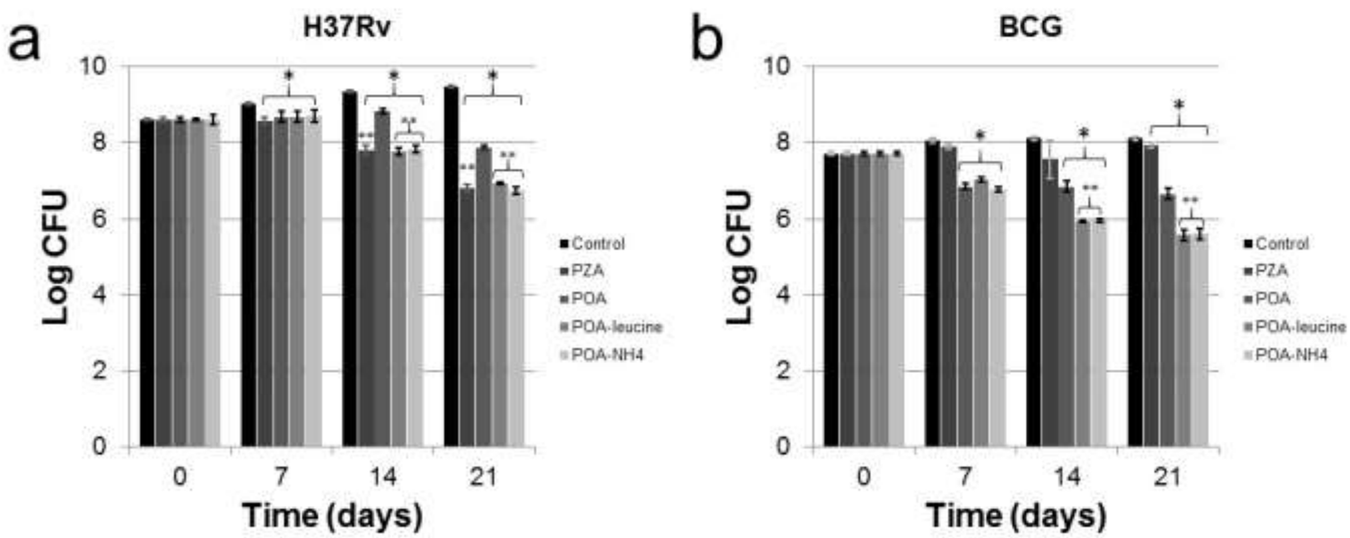

Antibacterial activity of POA salts: The antimicrobial effect of POA salts are shown in Figure 7. The effects of POA in various forms on the growth of *Mtb* (Figure 7a), strain H37Rv and attenuated *Mycobacterium bovis* (BCG, Figure 7b) are shown. At all times following the initiation of the experiment the drug treatments were significantly effective in killing *Mtb H37Rv* in comparison to the untreated control group. At 14 and 21 days the POA salt and PZA treated groups were statistically more effective in killing *MTb H37Rv* than the POA alone. Throughout the experiment PZA was statistically similar in effect to untreated control in terms of BCG. At all times following initiation of the experiment POA salts and POA alone were statistically more effective in killing BCG than either PZA or untreated control groups. At 14 and 21 days the POA salts were statistically more effective ($p<0.05$) than POA alone.

DISCUSSION

Elemental analysis and melting behavior of the reaction products indicated that the process successfully generated salts. Elemental analysis confirmed the identification of the salts, with the theoretical and experimental values within the margin of error. Melting point determination demonstrated a single melt phenomenon rather than separate effects due to the independent components of the construct. The melting point values were addressed more accurately and in comparison with POA in the subsequent thermal analysis.

Given the thermal profile of POA a low outlet temperature with respect to decomposition temperature was targeted while atomization parameters were chosen based on prior experience with spray drying other small molecules. [28]

Particle Morphology: Morphologically, the POA-leu particles resemble previously reported particles with moderate leucine content, possibly due to high initial droplet surface saturation during drying [29]. This results in earlier shell formation and larger, less dense particles. Such particles generally are more dispersible than smaller, denser particles.

POA-NH4 particles are corrugated in appearance with a hollow sphere, low density morphology. These particles exhibited an aerodynamic diameter that was greater than their geometric diameter. Given the aerodynamic diameter can be approximated as the product of the square root of the particle density and the geometric diameter [25], this suggests insufficient deaggregation. Spray drying yield of the ammonium salt (as a proportion of the nominal mass of 400mg) was low relative to the leucine (10% and 39%, respectively, for the same mass) and could be improved with further optimization. Wall losses do not scale proportionately to mass being spray dried. Increasing the mass spray dried would significantly increase yield. The POA-NH4 particles were more adherent to the spray drying collection vessel and would also experience significant increase in yield at high mass output since the vessel surfaces would be saturated. Consequently, recovery may be improved by increasing the batch size.

X-Ray Powder Diffraction: Data displayed distinct peaks for POA and both salts, before and after spray drying. The two salts had distinct and different crystalline peaks as bulk materials. The peak data for POA matched phase identification data for POA (PDF 00-27-1888)[30]. The two spray dried materials appear to have similar diffraction patterns, sharing the dominant peak location with that of POA. The POA-leu spectra show peaks throughout the spectrum that can be attributed as POA and leucine where they have been combined and POA in the ammonium salt for which the ion cannot be studied in the solid state. The lower intensity of the peaks in the salts with respect to POA alone indicate, in light of examining similar quantities of powder accounting for the proportion of the components, the potential for amorphous content. In addition, the variation in intensity of peaks within the spectrum that may be assigned to POA , particularly in the initial salts with respect to the POA alone may be an indication of polymorphism in the starting materials which has been observed by others for related salts [31]. However, the peaks in the spray dried material are more closely aligned both in angle and intensity to POA alone.

Thermogravimetric analysis: Thermogravimetric analysis shows differences in loss between the two salts as synthesized. The profile of POA-leu corresponds to the individual profiles for L-leucine and POA. POA-NH4 showed onset of loss at a lower temperature than POA itself, while POA-leu and POA had similar onset temperatures. ***Differential Scanning Calorimetry:*** POA showed decomposition at 223°C which is consistent with published values [32]. POA salts show similar thermal behavior before and after spray drying, indicating the process was not detrimental to the material. Melt peak onset occurred at temperatures slightly below those observed in the capillary method which is to be expected given the sensitivity of this method compared with capillary melting point method used to screen the salts immediately after manufacture.

Residual Moisture Determination by Karl Fischer Titration: Moisture content as determined by Karl Fischer is supported by thermogravimetric analysis curves which do not show noticeable mass loss corresponding to unbound water.

Aerodynamic Particle Size Distribution: Aerodynamic size is within appropriate range for lung deposition. POA-leu SD exhibited a smaller MMAD than POA-NH4 SD, potentially due to the lower density afforded by the initial surface saturation of the leucine salt as previously described. Smaller particles can be achieved through an optimized experimental design carefully modifying spray drying parameters. Methods for decreasing particle size include increasing the mass flow ratio between the atomizing gas and the liquid feed and decreasing the concentration of dissolved solids in the solution. Emitted dose for both powders was sufficient for efficient use in other studies.

Antibacterial activity of POA: As expected PZA had a high antibacterial effect on Mtb H37Rv but not on BCG, and POA was bactericidal for both strains, with higher effect on BCG than Mtb H37Rv. Interestingly, both POA salts were more bactericidal on the two bacterial strains than pure POA which supports the hypothesis that the salt form increases the killing effect. The bacteria were held under static conditions for up to 60 days, then pH changed to acid conditions to ensure the bactericidal action of PZA and POA. The two logarithm reduction achieved by the salts with respect to untreated control and benefits seen with respect to PZA and POA alone would be an enormous advantage when translated to the multiple drug regimen standard of care described earlier (EHRZ).

In order to understand the significance of the outcome of the antibacterial activity studies the effects of pH on the efficacy of POA can be explored further. The Zhang hypothesis, described earlier, is supported by experimental evidence. [16, 17] Paradoxically, after the initial deamination within the bacilli, the POA produced leaves the bacilli fairly readily. However, after the POA has re-entered the cell, it is eliminated by means of an efflux pump. Either POA traverses the cell membrane with comparative ease (as postulated after the deamination step) or it only traverses it with great difficulty (as postulated to account for its lethal accumulation within the cell). To get over this logical problem, it has been postulated that first that the charged POA molecule cannot easily pass through the cell membrane. After deamination, the $–NH_3$ molecule turns to ammonium (NH4.OH) on contact with cell water which then combines with the POA to form POA-NH_4. This uncharged salt should pass through the cell membrane with ease. In an acid environment, the dissociated POA ion from the salt would be protonated and would NOT diffuse through the cell membrane to accumulate within the cell.

An explanation for the appearance of PZA inactivity in culture was explained by McDermott & Tompsett in 1954 [33]. In these experiments, Tween-albumin or oleic acid-albumin liquid media were adjusted by addition of NaOH or HCl to a range of pH values between pH 4.5 and pH 8.0. It was clear that there was a great change in the MIC over the range of pH 6.0-5.5. The effect of pH on the activity of other potential anti tuberculosis drugs used in first line therapy is also relevant.

There are two possible explanations for the pH of active tuberculosis lesions being acidic. Firstly, because inflammation accompanied by anoxia tends to produce acid conditions by the accumulation of lactic acid [34] and secondly because counts of viable bacilli in sputum show that PZA treatment, given without any other anti-tuberculosis drugs in studies of early bactericidal activity, is bactericidal during the initial 14 days of treatment [35]. On average, 97% of the bacilli were killed in this study and there was no apparent alteration in the speed of the bactericidal action once it had started at about day 2. Thus, the great majority of the bacterial population that is being sampled in sputum is at a sufficiently acid pH for the PZA given in treatment to be clearly bactericidal. Since peak plasma concentrations are about 30 µg/ml PZA [36], these lesions must have a pH of less than 6.0 for the achievable PZA concentration in the lesions to be above the MIC. Multiplication of *M. tuberculosis* must be occurring because large numbers of bacilli are being excreted from the lungs in sputum.

Consequently, preparing salts of POA allows local modulation of pH sufficient based on the counterion to allow uptake of the drug and thereby to increase its activity against mycobacteria as demonstrated in the present study. Since the drug can be prepared in a form suitable for delivery as an aerosol to the lungs it is anticipated that this effect would be beneficial in local therapy when delivered by inhalation. Of the two salt forms prepared since both treated mycobacteria effectively POA-leu would be the best candidate for development based on its physicochemical properties and performance as an aerosol. However, both salts have physico-chemical properties (morphology) and performance (aerodynamic particle size and distribution and delivered dose) similar to those observed for other candidates such as capreomycin. [20, 21]

CONCLUSION

Pyrazinamide is a valuable drug in the treatment of *Mtb*. With new interpretations of the mechanism of action of PZA and its active moiety POA, new deployment strategies can be utilized to provide an adjunct pulmonary therapy to decrease the duration of treatment and improve the efficiency of the current drug regimen.

Both POA salts investigated were suitable for spray drying and their morphology and particle size was within the range suitable for pulmonary delivery. POA salt counterion selection impacts particle morphology for the same process conditions, potentially influencing aerosol performance.

Salts of POA were more effective in an in vitro evaluation of action against two mycobacteria. It has been demonstrated here that these salts can be prepared as respirable dry powders suitable for further evaluation in an animal model.

The immediate priorities for future work are further optimization of the spray drying process, performance of studies to evaluate the in vivo efficacy and tolerability of the POA salts in animals.

ACKNOWLEDGMENTS

We are grateful to Mr. J. Todd Ennis for assistance in obtaining X-ray powder diffraction data. Some of the data in this paper was presented in abstract at the American Association of Pharmaceutical Scientists Annual Meeting held in San Antonio, TX during November 2013.

REFERENCES

1. World Heath Organization, *Fact Sheet No. 104*2015.
2. Fox, W., *Whither short-course chemotherapy?* Br J Dis Chest, 1981. **75**(4): p. 331-57.
3. *Essentially of Pyrazinamide Workshop*. in *Stop TB Partnership Working Group on New Drugs*. 2011. Bethesda, MD.
4. Mitchison, D.A., *Role of individual drugs in the chemotherapy of tuberculosis.* Int J Tuberc Lung Dis, 2000. **4**(9): p. 796-806.
5. Lu, P., et al., *Pyrazinoic acid decreases the proton motive force, respiratory ATP synthesis activity, and cellular ATP levels.* Antimicrob Agents Chemother, 2011. **55**(11): p. 5354-7.
6. Cole, S.T., *Microbiology. Pyrazinamide--old TB drug finds new target.* Science, 2011. **333**(6049): p. 1583-4.
7. Shi, W., et al., *Pyrazinamide inhibits trans-translation in Mycobacterium tuberculosis.* Science, 2011. **333**(6049): p. 1630-2.
8. Kjellsson, M.C., et al., *Pharmacokinetic evaluation of the penetration of antituberculosis agents in rabbit pulmonary lesions.* Antimicrob Agents Chemother, 2012. **56**(1): p. 446-57.
9. Matthews, J., *IX. Pyrazinamide and isoniazid used in the treatment of pulmonary tuberculosis.* Am Rev Respir Dis., 1960. **81**: p. 348-351.
10. McKenzie, D., et al., *The effect of nicotinic acid amide on experimental tuberculosis of white mice.* J Lab Clin Med., 1948. **33**: p. 1249-1253.
11. Solotorovsky, M., et al., *3rd. Pyrazinoic acid amide; an agent active against experimental murine tuberculosis.* Proc Soc Exp Biol Med., 1952. **79**(4): p. 563-565.

12. Yeager, R.L., W.G. Munroe, and F.I. Dessau, *Pyrazinamide (aldinamide) in the treatment of pulmonary tuberculosis.* Am Rev Tuberc, 1952. **65**(5): p. 523-46.
13. McCune, R. and R. Tompsett, *Fate of Mycobacterium tuberculosis in mouse tissues as determined by the microbial enumeration technique. I. The persistence of drug-susceptible tubercle bacilli in the tissues despite prolonged antimicrobial therapy.* J Exp Med. , 1956. **104**: p. 737-762.
14. East African/British Medical Research Councils, *Controlled clinical trial of short-course (6-month) regimens of chemotherapy for treatment of pulmonary tuberculosis.* The Lancet, 1972. **299**(7760): p. 1079-1085.
15. Konno, K., F.M. Feldmann, and W. McDermott, *Pyrazinamide susceptibility and amidase activity of tubercle bacilli.* Am Rev Respir Dis, 1967. **95**(3): p. 461-9.
16. Zhang, Y. and D. Mitchison, *The curious characteristics of pyrazinamide: a review.* Int J Tuberc Lung Dis, 2003. **7**(1): p. 6-21.
17. Scorpio, A., et al., *Characterization of pncA mutations in pyrazinamide-resistant Mycobacterium tuberculosis.* Antimicrob Agents Chemother, 1997. **41**(3): p. 540-3.
18. Scheuch, G., et al., *Clinical perspectives on pulmonary systemic and macromolecular delivery.* Adv Drug Del Rev., 2006. **56**: p. 996-1008.
19. Smola, M., T. Vandamme, and A. Sokolowski, *Nanocarriers as pulmonary drug delivery systems to treat and to diagnose respiratory and non respiratory diseases.* Int J Nanomedicine., 2008. **3**: p. 1-19.
20. Garcia-Contreras, L., et al., *Inhaled large porous particles of capreomycin for treatment of tuberculosis in a guinea pig model.* Antimicrob Agents Chemother., 2007. **51**: p. 2830-2836.
21. Fiegel, J., et al., *Preparation and in vivo evaluation of a dry powder for inhalation of capreomycin.* Pharmaceutical Research, 2008. **25**(4): p. 805-11.
22. Tsapis, N., et al., *Direct lung delivery of para-aminosalicylic acid by aerosol particles.* Tuberculosis, 2003. **83**: p. 379-385.
23. Muttil, P., C. Wang, and A.J. Hickey, *Inhaled drug delivery for tuberculosis therapy.* Pharmaceutical Research, 2009. **26**(11): p. 2401-16.
24. Misra, A., et al., *Inhaled drug therapy for treatment of tuberculosis.* Tuberculosis (Edinb), 2011. **91**(1): p. 71-81.
25. Convention, U.S.P., *U.S. Pharmacopeia National Formulary 2011: USP 34 NF 29*2011: United States Pharmacopeial.
26. Srichana, T., G.P. Martin, and C. Marriott, *Dry powder inhalers: The influence of device resistance and powder formulation on drug and lactose deposition in vitro.* European Journal of Pharmaceutical Sciences, 1998. **7**(1): p. 73-80.
27. International Standards Organization, *Anaesthetic and respiratory equipment*, in *Nebulizing systems and components*2009.
28. Chuck, R.J. and U. Zacher, *Spray drying an aqueous solution of ammonium nicotinate;heating aftertreatment*, 2002, Google Patents.
29. Vehring, R., *Pharmaceutical Particle Engineering via Spray Drying.* Pharmaceutical Research, 2008. **25**(5): p. 999-1022.
30. JCPDS--International Centre for Diffraction Data American Society for Testing Materials, *Powder Diffraction File: Inorganic and organic*2001: JCPDS International Centre for Diffraction Data.
31. Prasad, K.D., et al., *Differential Cocrystallization Behavior of Isomeric Pyridine Carboxamides toward Antitubercular Drug Pyrazinoic Acid.* Crystal Growth & Design, 2015. **15**(2): p. 858-866.
32. Lewis, M.W., *Preparation of pyrazinoic acid*, 1954, Google Patents.
33. McDermott, W. and R. Tompsett, *Activation of pyrazinamide and nicotinamide in acidic environments in vitro.* Am Rev Tuberc, 1954. **70**(4): p. 748-54.

34. von Ardenne, M. and W. Kruger, *Local tissue hyperacidification and lysosomes.* Front Biol, 1979. **48**: p. 161-94.
35. Jindani, A., C.J. Dore, and D.A. Mitchison, *Bactericidal and sterilizing activities of antituberculosis drugs during the first 14 days.* Am J Respir Crit Care Med, 2003. **167**(10): p. 1348-54.
36. Ellard, G.A., *Absorption, metabolism and excretion of pyrazinamide in man.* Tubercle, 1969. **50**(2): p. 144-158.